Analysis of 3D Printing Materials as Potential Radiological phantoms of Lung Organs for Medical Imaging purposes

M. Yunianto[1*], F. Anwar[1], T. D. Ardyanto[2]

[1]Department of Physics, Universitas Sebelas Maret, Surakarta, Indonesia.
[2]Department of Clinical Pathology, Universitas Sebelas Maret, Surakarta, Indonesia.

ABSTRACT: Research has been conducted to analyze and characterize ten 3D printing materials as potential Radiological Phantoms of Lung Organs. Eight filaments of PLA, ABS, HIPS, Carbon, Nylon, TPU, PETG, and Wood were printed using an FDM type 3D printer, and two resins, PLA resin and Water washable resin, were printed using an SLA type 3D printer. The phantoms were printed with thickness variations of 3 mm, 6 mm, and 9 mm. 8 parameters were used to obtain the best material, namely material density, CT number, electron density (Ne), effective electron density (EDG), electron density per volume (EDV), effective atomic number (Zeff), material constituent elements, and elastic Modulus. Based on comparing the values of 8 parameters, the most potential to be used as phantom material for lung organs is PLA.

KEYWORDS: 3D printer, filament, radiology, phantom, lung

I. INTRODUCTION

The human body comprises various tissues and cavities with various physical shapes and radiological properties. In the process of radiodiagnostics, the absorbed dose given to all these tissues must be considered (Handoko *et al.*, 2018). In radiology, phantoms are used to measure the feasibility of certain radiological devices or as a medium in measuring radiation doses, especially for brachytherapy. Phantom is a mock object of human anatomy that has functions, among others, as a medium for testing image quality and dose absorption in radiology equipment feasibility testing activities and irradiation media in radiotherapy planning. Today's Phantoms are expensive and imported goods from developing countries that make phantoms (Mufida *et al.*, 2020). The price of phantoms is relatively high (Giron *et al.*, 2019), whereas anatomically similar phantoms are already commercially available. The development of 3D-printed phantoms is a solution option because it allows the formation of geometric designs that are identical to the shape of human body tissues at a relatively affordable cost. These phantoms are usually used for image quality assessment, providing detailed anatomy and attenuation properties comparable to real human tissue but at a high cost.

Physical anthropomorphic 3D phantoms are needed and expected to produce realistic images of organ tissue patterns; this is important for investigating and detecting nodules and knowing the performance of image processing algorithms Ikejimba *et al.*, (2017). To be successful in designing and manufacturing lung phantoms, 3D printer materials need to be studied to determine the radiological characteristics, material composition, and physical characteristics as a lung substitute for X-ray imaging, especially to obtain 3D printer materials that are compatible with the lung organ, using low exposure parameters with optimal results and low cost.

A good phantom should have anatomical design, radiological characteristics, and material composition identical to the characteristics of human organs or tissues (Zhang *et al.*, 2019). In radiotherapy planning, the CT number and electron density values need to be considered for limiting the radiation irradiation area; because of this influence, the electron density parameter needs to be considered in making phantoms (Purwatiningish & Lesmana, 2019).

By utilizing technological advances, a more affordable alternative to making phantoms can be made using a 3D printer. Making diagnostic phantoms using 3D printing has several advantages, such as more flexible design, cost reduction, and knowledge of organ design from standard reference objects. In addition, complex or fine-detail structures can be created through 3D printer techniques (Giron *et al.*, 2019).

The proposed methods include using eight parameters, consisting of the CT number, material density, relative electron density, electron density per gram (EDG), electron density per volume (EDV), effective atomic number, material composition, and mechanical properties of the material. These eight parameters are used to evaluate ten 3D printer materials, which are expected to obtain materials with the most potential as lung phantom materials.

II.   RELATED WORKS

Research on the development and manufacture of phantoms with the application of 3D printing has been carried out by several researchers with different applications, developed phantoms using 3D printer EDEN 500V to make liver phantoms using polymethylmethacrylate material obtained results that have density and HU values close to human liver organs (Gear *et al*, 2014). Park *et al*. (2016) developed a breast bolus phantom for breast cancer therapy with the material clear PLA with a volume of 200 cc and 300 cc. The breast bolus phantom was compared with a commercial bolus (Super-Flex bolus), and then dose measurements were made using a MOSFET dosimeter, the results obtained were that the clear PLA material had almost the same characteristics as the Super-Flex bolus.

Alssabagh *et al*. (2017) developed a thyroid phantom for medical dosimetry and image quality testing using five 3D printer materials, namely Polylactic Acid (PLA), Acrylonitrile Butadiene Styrene (ABS), Polyethylene Terephthalate Glycol (PETG), Thermoplastic Elastomers (TPE) and Polyamide (PA), the parameters tested were constituent composition, attenuation coefficient and CT number. The best material for thyroid phantom development was found to be PLA.

Ivanov *et al*. (2018) developed a breast phantom using ABS, Brick, Hybrid, Nylon, PET-G, PLA, PMMA, and PVA materials. Linear attenuation coefficient and material composition were compared for each material; ABS is the best material for breast adipose material. Manufacture of anthropomorphic thorax phantoms for medical imaging purposes (Hazelaar *et al*, 2018) and development of anthropomorphic chest phantom in radiotherapy applications (Zhang *et al*, 2019).

Lung vascular system (Giron *et al*, 2019) and tested it by comparing the test results with commercial anthropomorphic phantoms and patient data. One of the 3D printer materials used in this study is the Visijet EX200. The results obtained from this study were that the attenuation of the phantom from the Visijet EX200 was higher than the attenuation observed in patients. In contrast, that of the commercial phantom was lower.

Fujibuchi (2021) made a Neonatal chest phantom using PLA for gypsum and urethane. Tests were carried out using X-Ray to compare with human body X-Ray results visually; CT imaging was carried out to determine the CT number value compared to Original CT images; the results had almost the same value at a lower cost. Pelvic phantom (Giacometti *et al*, 2021) is compared with commercial pelvic phantoms using PLA material. This study aims at dose calculation and verification in Stereotactic Ablative Radiation Therapy (SABR). This phantom has successfully validated SABR using various detectors.

Lung phantoms with variations in phantom infill where the results showed that the greater the infill value, the greater the HU value of the phantom. Also obtained are phantoms with accuracy in organ geometry, image texture, and attenuation values (Meilinda & Arifin, 2014).

III.   MATERIALS AND METHODS/METHODOLOGY/EXPERIMENTAL PROCEDURE

Phantom designs with thickness variations for ten 3D printer materials were subjected to several tests. Radiological testing begins with data collection in the form of images using a CT-Scan aircraft, then determining the value of HU or CT-number using RadiAnt DICOM Viewer software and calculating material density, relative electron density, electron density per gram (EDG), electron density per volume (EDV), effective atomic number, test using SEM-EDX to determine the composition of material elements and material compressive test using Universal Testing Machine (UTM) as presented in Figure 1. All material parameters tested are compared with the lung parameters of ICRU-44 (1989).
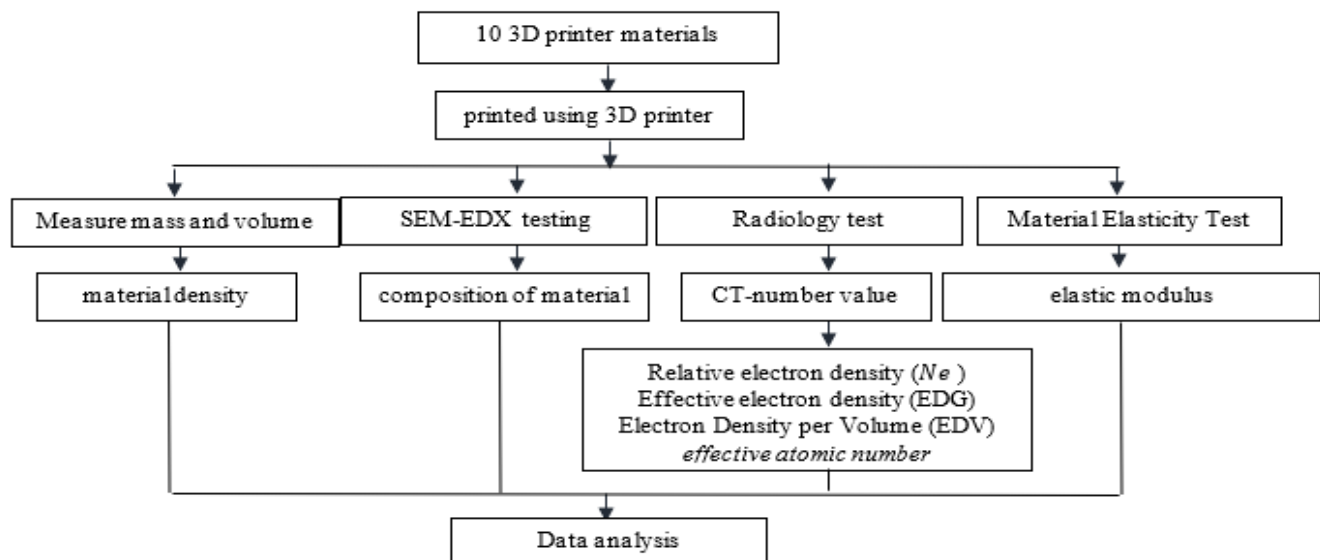
Figure 1: Schematic Diagram of Proposed Method

A. *Preparation of phantom material samples*

The initial stage of the research was manufacturing samples from 10 phantom materials that would be evaluated as materials for lung phantoms. These materials are eight filaments of PLA, ABS, HIPS, Carbon, Nylon, TPU, PETG, and Wood and two resins: PLA resin and Water washable resin. The materials are made in 3 mm, 6 mm, and 9 mm thickness variations with dimensions, as shown in Figure 2.

The 10 materials are then printed using various types of 3D printers according to the characteristics of the material; Table 1 is the type of printer used for the phantom material printing process.
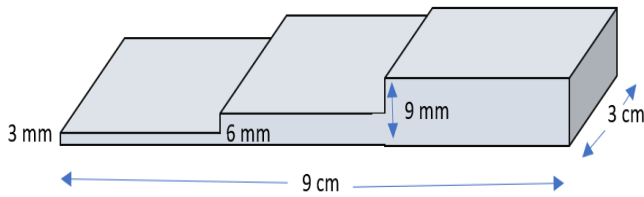
Figure 2: Design of phantom material samples

Table 1: Merk and types of 3D printers for printing phantom materials

Material	Printer Merk	Printer type
PLA	Ender 3	FDM
ABS	modified anycubic 3 mega with enclosure box	FDM
Carbon	IMA 3030 pro	FDM
TPU	IMA 2020, direct extruder	FDM
PETG	Cr-10	FDM
Wood	Anet4	FDM
HIPS	modified anycubic 3 mega with enclosure box	FDM
Nylon	IMA 3030 pro	FDM
PLA resin	Anycubic Photon	SLA
Water washable resin	Anycubic Photon	SLA

B. *Density value*

Ten materials that have been printed are then calculated with the density value of each, the mass of each material is measured using digital scales, and the volume is measured using a measuring cup. Determination of the material density value can be calculated using Eqn. 1.

$$\rho = \frac{m}{V} \tag{1}$$

C. *Image data collection using CT-Scan*

Radiological tests using CT-Scan were conducted to determine the CT-number value of the tested sample material. Before radiological testing begins, CT-Scan aircraft specifications are recorded and documented as performance information from the CT-Scan aircraft. The CT-Scan aircraft is prepared or warmed up for approximately 10 minutes. The tested sample is placed on the patient table and positioned using the laser beam on the X-ray aircraft feature. The sample position is placed vertically. The CT-Scan aircraft ready to use is then set for the type of examination. The tube voltage (kV) value is 130 kV and 180 mA for the tube current setting. In addition to setting kV and mAs, the slice thickness was also set

at 0.8 mm. Next, the sample was exposed to obtain the program image.

The tomogram image seen on the monitor screen is adjusted to the area of irradiation, which adjusts the overall area of the sample. It was then reexposed with the same examination type, kV, mAs, and slice thickness settings as when exposing the program image. The image data in the DICOM file obtained was burned, i.e., transferred or copied to a CD cassette.

D. *CT-number*

CT-Number was searched using the Region of Interest (ROI) technique using RadiAnt DICOM Viewer software. ROI was searched for 9 points then the results were averaged. CT-Number values were compared with Gammex-467 phantom data, ICRU Report 46 data (Saito & Sagara, 2017), and CT-Number data from several references (McGarry *et al*, 2020).

E. *Relative electron density (Ne)*

Relative electron density is the number of electrons in a particular region. Electron density must be considered when selecting phantom material because it can affect image quality and dose distribution in radiotherapy. In radiotherapy treatment planning, electron density accounts for the heterogeneity of body tissues. Such heterogeneity can optimize dosimetry when planning radiotherapy. The relative electron density (Ne) is determined through Eqns. 2 and 3 (Guswantoro *et al*, 2020).

$$N_e = 1{,}052 + 0{,}00048\,N_{CT} \tag{2}$$

Eqn. 2 calculates the electron density of a material with a CT number greater than 100. CT numbers smaller than 100 can be calculated with Eqn. 3 as follows:

$$N_e = 1{,}000 + 0{,}001\,N_{CT} \tag{3}$$

where N_e: Relative Electron Density, N_{CT}: CT number (HU), the attenuation coefficient of a material must be proportional to its electron density value N_e.

F. *Effective electron density (EDG)*

Electron density ρ_e (number of electrons per gram) for all materials is calculated using the composition of each constituent element (Akhlagi *et al*, 2015).

$$\rho_{e(EDG)} = N_A \sum \frac{w_i Z_i}{A_i} \tag{4}$$

where N_A is Avogadro's number and w_i, Z_i, and A_i are each atom's weight fraction, atomic number, and atomic mass.

G. *Electron density per volume (EDV)*

Electron density per volume (EDV) is used to explain the interaction between photons and lungs in volume size; EDV is an important parameter obtained using the equation (Chang *et al*, 2012).

$$\rho_{e(EDV)} = \rho_{e(EDG)} \times \rho \tag{5}$$

where $\rho_{e(EDV)}$ is the electron density per volume, $\rho_{e(EDG)}$ is the electron density per gram, and ρ is the density of the material.

H. *Effective atomic number (Zeff)*

In medical physics, evaluating the amount of radiation represented in ionizing radiation is important. The energy

transmitted through photon interactions in the composite substance cannot represent the atomic number uniquely in the entire energy region. This number in the composite substance is called the effective atomic number (Kaginelli *et al.*, 2009). The effective atomic number is the average atomic number for a mixture of materials, a measure of the electrostatic interaction between negatively charged electrons and positively charged protons in the atom, Effective atomic numbers are useful for understanding why electrons far from the nucleus are bound much more weakly than those closer to the nucleus. Eqn. 6 determines the magnitude of the effective atomic number (Akhlagi *et al.*, 2015).

$$Z_{eff} = \frac{\sum \frac{w_i Z_i}{A_i}}{\sum \frac{w_i}{A_i}} \qquad (6)$$

I. Composition of materials

SEM-EDX test aims to determine the composition of the constituent materials of the phantom material; before testing, the material is cut to size on the SEM testing photo machine in the form of a box of 3 mm x 3 mm x 1 mm. Material samples to be tested are placed on a photo SEM testing machine; testing is carried out with an acceleration voltage setting of 15.00 KV, 300 x magnification.

J. Mechanical properties of a material

The mechanical properties of a material that can provide basic information on the strength of a material and as support for the specification data of a material can be carried out by carrying out a pressure test. The compression test measures a material's strength against mechanical stress. Pressure tests can be carried out using the Universal Testing Machine (UTM) (Fatima *et al.*, 2021). The Equation used in the compressive strength test is as in Eqn. 7.

$$Y = \frac{F/A}{\Delta l / l_o} \qquad (7)$$

where σ = Pressure/Force (N), A = Surface area, Δl = change in length and (m) l_0 = original length (m).

IV. RESULTS AND DISCUSSION

A. Material Phantom

Starting with the design for the printing process of phantom materials from filament and resin 3D printing, ten phantom materials, as for the ten materials are eight filaments of PLA, ABS, HIPS, Carbon, Nylon, TPU, PETG, and Wood, and two resins, namely PLA resin, and Water washable resin. The materials were made in 3 mm, 6 mm, and 9 mm thickness variations with the dimensions shown in Figure 2.

Figure 3: Molding results of 10 samples of 3D printing materials

The printing process of these materials uses various brands of printers to adjust the conditions of the material, especially nozzle temp and base plate temp. Each material has different specifications, types, and types of 3D printers used in the printing process in Table 1. Figure 3 is a phantom of printing results for ten types of 3D printer materials.

In determining the density of the material, 10 materials were measured, and calculated the mass value divided by volume; data collection was carried out three times, as shown in Figure 4. Eqn. 1 to determine the density value of the material. The results of the density value calculation are presented in Table 2 and compared with the lung density value from various sources.

(a)   **(b)**
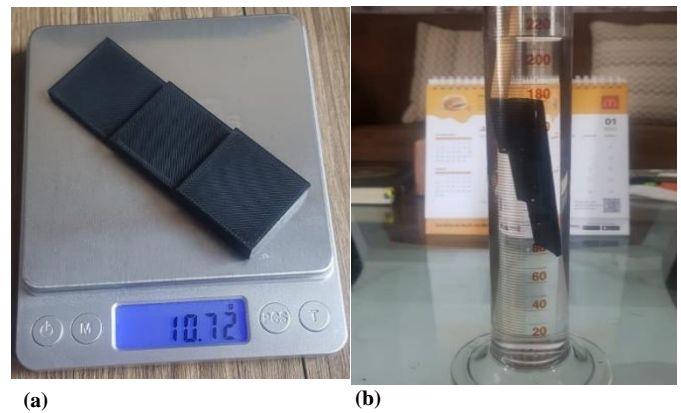
Figure 4: Measuring (a) Mass of the material (b) Volume of the material

Table 2: Density values of lung phantom and standard phantom materials

Material	Density (gr/cm³)
LN-300 lung (Gamex, 2015)	0.300
Lung (ICRU-44, 1989)	0.260
PLA	0.567
ABS	0.572
Carbon	0.556
TPU	0.616
PETG	0.662
wood	0.556
HIPS	0.586
Nylon	0.571
PLA *resin*	1.204
Water washable resin	1.293

Based on the material density values from Table 2, it can be seen that the density of the ten material samples is greater than the density of the standard phantom and the International Commission on Radiation Units and Measurements (ICRU) database. The closest materials are carbon and PLA filaments. The density of the material can change based on the mass of the sample because, for the manufacture of these samples, the 3D printer printing process uses 100% infill; if the infill value is varied by a certain percentage, a sample that has the same density as the lung will be obtained.

B. CT number

Testing 10 samples of 3D printer materials to determine the CT number value using CT-Scan brand Siemens emotion 16. This study was conducted using the abdominal examination mode. The exposure setting on the CT-Scan was set at 130 kV and 23 mAs, which is the usual setting for patient examination. The automatic setting on the CT-Scan system refers to patient protection, where the radiation dose needs to be controlled within safe limits. The greater the current strength set, the greater the radiation dose the object will receive.

CT number and standard deviation values in the same slice can have different ROI results even though they are treated with the same ROI shape and size, so it is necessary to take repeated data for the same slice. The difference in image slices is what makes the CT number and standard deviation different because each image slice records different X-ray attenuation; Table 3 is the average of CT number retrieval for thickness variations.

Table 3: CT number data for ten 3D printing material samples

Material	CT number (HU)	SD (HU)
PLA	-660.61	14.67
ABS	-632.93	2.85
Carbon	-656.87	10.18
TPU	-598.62	17.11
PETG	-617.57	16.37
wood	-636.05	5.05
HIPS	-635.74	9.61
Nylon	-634.67	7.45
PLA *resin*	103.93	6.13
Water washable resin	156.39	10.55

The standard deviation determines the noise level of the image. Random variations of pixel values in an image are known as noise. The image quality decreases as the noise level increases (Khoramian *et al*, 2019). Although the area of the ellipse and the number of pixels depicted are the same, the CT number and the noise magnitude may vary. The treatment of changing the gantry angle from 00 to 300 in the range of 50 increases the 2% - 50% standard deviation of the noise; this difference is caused by variations in the thickness of radiology image fragments that are too thin (Listyani *et al.*, 2021). Three main factors affect noise in images, the first factor is quantum noise, which is determined by X-ray fluctuations or the number of X-ray photons detected (Seeram, 2016).

CT number values for several references, standard lung phantoms, and the ICRU database are presented in Table 4. When the CT number values in Table 3 are compared with the data in Table 4, out of 10 phantom material samples, eight

materials from the filament are close to the existing standard. However, PLA is closer to the standard value than the other material samples.

Table 4: CT number of the lung from several references

Reference	CT number (HU)
Gamex, 2015	-684.9
Yunus & Murtala, 2010	-500 to -700
Sari et al, 2018	-300 to -800
ICRU, 1989	-750 to -950

C. Electron Density (Ne)

The linear attenuation coefficient is affected by several things, such as tissue composition and its density in each voxel of the patient. Electron density affects X-ray attenuation or CT number. Electron density can be calculated using Eqns. 2 and 3. Electron density in the sample obtained and in the standard phantom as in Table 5 Electron density is calculated from each material's average CT number value.

Table 5: Electron density of each sample and standard phantom

Material	Electron Density
LN-300 lung (Gamex, 2015)	0.290
PLA	0.339
ABS	0.367
Carbon	0.343
TPU	0.401
PETG	0.382
Wood	0.364
HIPS	0.364
Nylon	0.365
PLA *resin*	1.102
Water washable resin	1.137

The relative electron density for PLA filament has the lowest value, while WWR material has the highest value; this corresponds to the CT number value where PLA has the smallest value while WWR has the largest value; CT number and electron density have a linear relationship. The CT number of a material or material is proportional to its electron density; this happens because the greater the electron density, the greater the possibility of X-ray interaction, namely, the higher the attenuation.

The electron density value is analyzed as the value that is close to the electron density value of the Gammex 467 phantom. The material can become a phantom if the difference between the values obtained from the research results and the reference is small, less than 0.1. Table 6 represents the potential of 3D printing materials as radiology phantom materials based on electron density values; it can be seen from the value that has the greatest potential is PLA filament.

Table 6: Potential of 3D printing materials as radiology phantoms based on Ne value and comparison with Ne standard

Material	N_e	Difference in value
LN-300 lung (Gamex, 2015)	0.290	-
PLA	0.339	0.049
ABS	0.367	0.077
Carbon	0.343	0.053
TPU	0.401	0.111
PETG	0.382	0.092
wood	0.364	0.074
HIPS	0.364	0.074
Nylon	0.365	0.075
PLA *resin*	1.102	0.812
WW resin	1.137	0.847

D. Effective electron density (EDG)

Based on the difference in effective electron density values between material samples and lung standards based on ICRU-44, according to Table 7, Carbon, Nylon, and PLA materials have the smallest difference. However, Carbon and Nylon have negative values, meaning the electron density value is lower. EDG value is strongly influenced by the chemical formula of the material, which depends on the atomic number and mass number of the constituents.

Table 7: Effective electron density values of sample materials and lung standards

Material	EDG (e^-/g)	Differences (e^-/g)
Lung (Saito & Sagara, 2017)	3.350×10^{23}	-
PLA	4.334×10^{23}	9.844×10^{24}
ABS	4.515×10^{23}	1.165×10^{23}
Carbon	3.010×10^{23}	-3.400×10^{24}
TPU	2.709×10^{23}	-6.410×10^{24}
PETG	4.650×10^{23}	1.300×10^{23}
wood	5.016×10^{23}	1.666×10^{23}
HIPS	4.515×10^{23}	1.165×10^{23}
Nylon	3.960×10^{23}	6.100×10^{24}
PLA *resin*	4.334×10^{23}	9.844×10^{24}
WW resin	$4,603 \times 10^{23}$	1.253×10^{23}

E. Electron density per volume (EDV)

Electron density per volume shows the value of the number of electrons per gram (EDG) multiplied by the density of the material. In contrast, the EDV values for each material are presented in Table 8.

Table 8: EDV values of sample materials and lung standards

Material	EDV (e^-/cm^3)	Differences (e^-/cm^3)
Lung (ICRU, 1989)	8.610×10^{22}	-
PLA	1.469×10^{23}	6.082×10^{22}
ABS	1.657×10^{23}	7.960×10^{22}
Carbon	1.032×10^{23}	1.714×10^{22}
TPU	1.086×10^{23}	2.225×10^{22}
PETG	1.776×10^{23}	9.153×10^{22}
Wood	1.823×10^{23}	9.648×10^{22}
HIPS	1.646×10^{23}	7.825×10^{22}
Nylon	1.445×10^{23}	5.844×10^{22}
PLA *resin*	4.776×10^{23}	3.915×10^{23}
WW resin	5.233×10^{23}	4.373×10^{23}

Based on the data on the difference in EDV values for lung materials and standards, it can be seen that the difference is relatively large for all samples; the values that are close to the standard are Carbon and TPU filaments; this EDV value can allow it to change even though the type of material is the same because it also depends on the density of the material, the density of the material can be changed by adjusting the density of the material, for 3D printer materials it can be adjusted through the percentage value of infill.

F. Effective Atomic Number (Zeff)

Effective atomic number (Zeff) is the average atomic number for a mixture of materials; a material has an effective atomic number that shows the electrostatic interaction between negatively charged electrons and positively charged protons in the atom. It can be seen from the difference in the value of wood material has the least difference among other materials, so it can be interpreted that Wood has an average atomic number that is close to the average atomic number for the lung, the Zeff values for each material are presented in Table 9.

Table 9: Effective atomic number (Zeff) values of material samples and lung standards

Material	Z_{eff}	Differences
Paru (ICRU, 1989)	3.43	-
PLA	5.66	2.23
ABS	11.08	7.65
Carbon	6.04	2.61
TPU	1.29	2.14
PETG	12.40	8.97
Wood	4.36	0.93
HIPS	11.08	7.65
Nylon	6.02	2.59
PLA *resin*	5.66	2.23
WW resin	10.98	7.55

G. Composition of materials

Materials tested using SEM-EDX, EDX (Energy Dispersive of X-Ray Spectroscopy) section to determine the composition of the constituents of 3D Printer materials. The treatment given to the material sample is that the sample is cut with a size of 3 mm x 3 mm and 1 mm to facilitate placement on the photo testing machine; the placement of the material on the SEM-EDX is shown in Figure 5. The test results of 10 samples using SEM EDX for the PLA material sample are presented in Figure 6 to analyze the composition elements of the material and also presented in Table 10.
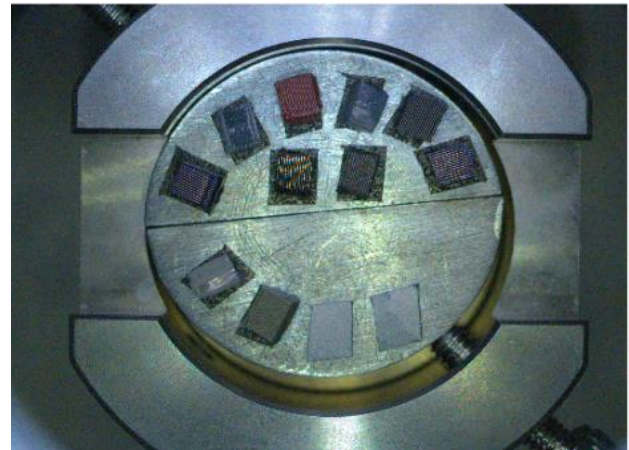
Figure 5: Placement of 10 samples of 3D printing materials on SEM-EDX
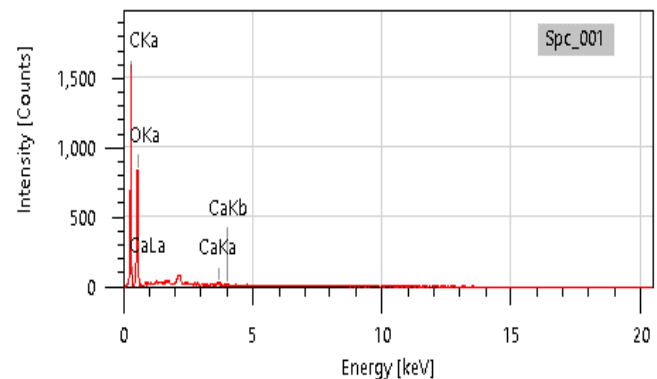
Figure 6: Graph of SEM-EDX test results for PLA material

Table 10: The composing elements of sample material and lung standard (ICRU-44)

Material	The composing elements (weight fraction)						
	H	C	N	O	Na	Si	Ca
Lung (ICRU, 1989)	0.103	0.105	0.031	0.749	0.002		
PLA		0.466		0.526			0.082
ABS		1.000					
Carbon		0.729		0.268		0.076	
TPU		0.640		0.360			
PETG		0.591		0.409			
Wood		0.472		0.520		0.077	
HIPS		1.000					
Nylon		0.743		0.257			
PLA *resin*		0.646		0.354			
WW resin		0.557		0.443			

H. Elastic Modulus of materials

Ten samples of phantom materials were tested using a Universal Testing Machine (UTM) brand Gotech Testing Machine Inc model GT-7001-LC 50. The test results are in the form of a graph of pressure against the length of the object that is depressed or exposed to loads from the machine (extension). Information on the maximum load and extension at the maximum time is also displayed on the test results of the elastic Modulus of the tested material obtained from the test results, as presented in Table 11.

Table 11: Elastic modulus values of phantom and standard materials

Material	Elastic Modulus (Pa)
Lung (Sicard et al, 2018)	1.87×10^3
Lung (McKee et al, 2011)	$(1.4$-$6.1) \times 10^3$
Porcine lung tissue (Jansen et al, 2015)	2.55×10^3
Porcine lung tissue (Cui et al, 2011)	3.68×10^3
PLA	1.05×10^9
ABS	9.40×10^9
Carbon	10.61×10^9
TPU	13.00×10^9
PETG	3.30×10^9
wood	0.19×10^9
HIPS	0.25×10^9
Nylon	10.35×10^9
PLA resin	1.50×10^9
WW resin	$9,69 \times 10^9$

In manufacturing phantoms for radiology, the elastic modulus component is needed to select materials with the best physical quality as phantom materials.

The elastic modulus value of each material, when compared to the standard lung material, has a much greater value; the greater elastic modulus value does not determine the best physical parameters because the greater elastic Modulus indicates that the object is more rigid. Of the 10 phantom materials having a large modulus leads to a rigid material, which has the smallest elastic Modulus of the 10 phantom materials, Wood.

I. Lung phantom potential of 3D printing materials

The best 3D printing phantom material from 10 materials is determined from several parameters, both physical properties of the material and radiological characteristics. Through the value of each parameter, the potential of 3D printing materials as phantom materials is shown in Table 12.

Based on the data from Table 12, the materials that have the potential as 3D printing materials for lung phantoms are PLA and Carbon; PLA has the CT number value, electron density, and constituent elements that are closest to the lung. These three components are the most important in making a phantom. Carbon has density, EDG, and EDV values closest to the lung; the value of density and EDV depends on the density of the material; the density value can change based on the mass of the sample with a fixed volume.

In printing phantom samples using a 3D printer using 100% infill, if a certain percentage varies the value of this infill, the density value of the material will change. It can be done to obtain samples with the same density as the lung.

Table 12: Potential of 3D printing materials as lung phantom materials

Parameters	Ranking of potential 3D printing materials for lung phantoms									
Density	Carbon	Wood	PLA	Nylon	ABS	HIPS	TPU	PETG	PLA resin	WWR resin
CT *number*	PLA	Carbon	Wood	HIPS	Nylon	ABS	PETG	TPU	PLA resin	WWR resin
N_e	PLA	Carbon	Wood	HIPS	Nylon	ABS	PETG	TPU	PLA resin	WWR resin
EDG	Carbon	Nylon	PLA	ABS	HIPS	PLA resin	WWResin	PETG	Wood	TPU
EDV	Carbon	TPU	Nylon	PLA	HIPS	ABS	PETG	Wood	PLA resin	WWR resin
Z_{eff}	wood	TPU	PLA	PLA resin	Nylon	Carbon	WW resin	ABS	HIPS	PETG
Composition of elements	PLA	Wood	WW resin	PEGT	TPU	PLA resin	Carbon	Nylon	ABS	HIPS
Elastic modulus	Wood	HIPS	PLA	PLA resin	PETG	ABS	WW resin	Nylon	Carbon	TPU

While the EDG value of Carbon is smaller than the EDG of the lung organ even though it has the closest value, the EDG value is a factor that affects the degree of attenuation of X-rays, the interaction of radiation with the material does not absorb radiation energy but rather absorbs some of the intensity of electromagnetic radiation, so if the EDG value is smaller, the intensity absorption becomes smaller than the lung organ. Based on comparing the values of the eight parameters and the analysis related to the parameter values, the most potential of the ten 3D printing materials to be used as a phantom material for the lung organ is PLA.

V. CONCLUSION

Eight filaments of PLA, ABS, HIPS, Carbon, Nylon, TPU, PETG, and Wood and two resins, PLA resin and Water washable resin, have characterized ten 3D printing materials as potential lung phantom manufacturing materials. 10 parameters were used to obtain the best materials, material density, CT number, Electron Density (Ne), Effective Electron Density (EDG), Electron Density per Volume (EDV), Effective Atomic Number (Zeff), material constituent elements, and elastic Modulus. PLA is the most potential material used as a lung organ phantom for Lung cancer Diagnosis and Therapy.

AUTHOR CONTRIBUTIONS

M. Yunianto: Conceptualization, Methodology, phantom design, research and analysis, Writing – original draft, Writing – review & editing. **F. Anwar:** Methodology, Material research dan analysis, Writing – original draft, Writing – review & editing. **T.D. Ardiyanto:** Methodology, Radiological research and analysis, Writing – review & editing.

REFERENCES

Akhlaghi, P. ; H. M. Hakimabad and L. R. Motavalli. (2015). Determination of tissue equivalent materials of a physical 8-year-old phantom for use in computed tomography. Radiation Physics and Chemistry, 112: 169-176. https://doi.org/10.1016/j.radphyschem.2015.03.030.

Alssabagh, M.; A. A. Tajuddin; M. A. Manap and R. Zainon. (2017). Evaluation of 3D printing materials for fabrication of a novel multi-functional 3D thyroid phantom for medical dosimetry and image quality. Radiation Physics and Chemistry, 135, 106-112 https://doi.org/10.1016/j.radphyschem.2017.02.009.

Chang, K. P.; S. H. Hung; Y. H. Chie; A. C. Shiau and R. J. Huang. (2012). A comparison of physical and dosimetric properties of lung substitute materials. Medical physics, 39(4): 2013-2020. https://doi.org/10.1118/1.3694097.

Cui, J.; C. H. Lee; A. Delbos; J. J. McManus and A. J. Crosby. (2011). Cavitation rheology of the eye lens. Soft Matter, 7(17): 7827-7831. https://doi.org/10.1039/C1SM05340J.

Danail, I.; B. Kristina; B. Ivan; P. Peycho; M. Giovanni; R. Paolo; D. L. Francesca; S. Antonio; V. Janne; B. Hilde; B. Alberto and B. Zhivko. (2018). Suitability of low density materials for 3D printing of physical breast phantoms. Physics in Medicine & Biology, 63(17): 175020 https://doi.org/10.1088/1361-6560/aad315.

Fatima, F.; C. I. Irgananda; K. A. Wulan and F. A. Tabatya. (2021). Kekuatan Tekan Model Gigi Berbahan Dasar Self-Cured Acrylic Sebagai Media Pembelajaran Keterampilan Klinis Prostodonsia. E-Prodenta Journal of Dentistry, 5(2): 496 - 505. http://dx.doi.org/10.21776/ub.eprodenta.2021.005.02.6.

Fujibuchi, T. (2021). Investigation of a method for creating neonatal chest phantom using 3D printer. In Journal of Physics: Conference Series, 1943(1): 012056 https://doi.org/10.1088/1742-6596/1943/1/012056.

Gamex (A Sun Nuclear Company). (2015). CT Electron Density Phantom. https://www.sunnuclear.com/documents/datasheets/gammex/ct_electron_density_phantom.pdf..

Gear, J. I.; C. Long; D. Rushforth; S. J. Chittenden; C. Cummings and G. D. Flux. (2014). Development of patient-specific molecular imaging phantoms using a 3D printer. Medical Physics., 41: 082502. https://doi.org/10.1118/1.4887854.

Giacometti, V.; R. B. King; C. McCreery; F. Buchanan; P. Jeevanandam; S. Jain; A. R. Hounsell and C.K. McGarry. (2021). 3D-printed patient-specific pelvis phantom for dosimetry measurements for prostate stereotactic radiotherapy with dominant intraprostatic lesion boost. Physica Medica, 92: 8-14. https://doi.org/10.1016/j.ejmp.2021.10.018.

Giron, H. I.; J. M, den Harder; G. J. Streekstra; J. Geleijns and W. J. Veldkamp. (2019). Development of a 3D printed anthropomorphic lung phantom for image quality assessment in CT. Physica Medica, 57: 47-57. https://doi.org/10.1016/j.ejmp.2018.11.015.

Guswantoro, T.; A. S. Supratman and I. S. Asih. (2020). Karakterisasi Alginat Sebagai Bahan Setara Dengan Jaringan Lunak Untuk Radioterapi. EduMatSains: Jurnal Pendidikan, Matematika dan Sains, 4(2): 125-138. https://doi.org/10.33541/edumatsains.v4i2.1378.

Handoko, A.; H. Hidayatullah; E. Hidayanto and V. Richardina. (2018). Analisis keakuratan verifikasi dosis dengan menggunakan perbandingan phantom standar dan phantom replica. Youngster Physics Journal, 7(1): 1-10. https://ejournal3.undip.ac.id/index.php/bfd/article/view/20857

Hazelaar, C.; M. V. Eijnatten; M. Dahele; J. Wolff; T. Forouzanfar; B. Slotman and W.F.A.R. Verbakel. (2018). Using 3D printing techniques to create an anthropomorphic thorax phantom for medical imaging purposes. Medical Physics, 45: 92-100. https://doi.org/10.1002/mp.12644

ICRU—International Commission on Radiation Units and Measurements. (1989). Tissue substitutes in radiation dosimetry and measurement, ICRU Report No. 44, os-23, 1. https://www.icru.org/report/tissue-substitutes-in-radiation-dosimetry-and-measurement-report-44/

Ikejimba, L. C.; C. G. Graff; S. Rosenthal; A. Badal, B. Ghammraoui, J. Y. Lo, and S. J. Glick. (2017). A novel physical anthropomorphic breast phantom for 2D and 3D x-ray imaging. Medical Physics, 44: 407-416. https://doi.org/10.1002/mp.12062.

Jansen, L. E.; N. P. Birch; J. D. Schiffman; A. J. Crosby and S. R. Peyton. (2015). Mechanics of intact bone marrow. Journal of the Mechanical Behavior of Biomedical Materials, 50: 299-307. https://doi.org/10.1016/j.jmbbm.2015.06.023.

Kaginelli, S. B.; T. Rajeshwari; B. R. Kerur and A. S. Kumar. (2009). Effective atomic numbers and electron density of dosimetric material. Journal of Medical Physics/Association of Medical Physicists of India, 34(3): 176. https://doi.org/10.4103%2F0971-6203.54853.

Khoramian, D.; S. Sistani and R. A. Firouzjah. (2019). Assessment and comparison of radiation dose and image quality in multi-detector CT scanners in non-contrast head and neck examinations. Polish Journal of Radiology, 84: e61-e67. https://doi.org/10.5114/pjr.2019.82743.

Listiyani, I. L.; A. Nismayanti; M. Maskur; K. Kasman; M. S. Ulum and A. R. Rahman. (2021). Analisis Noise Level Hasil Citra CT-Scan Pada Phantom Kepala Dengan Variasi Tegangan Tabung Dan Ketebalan Irisan, Gravitasi, 20(1): 5 - 9. https://doi.org/10.22487/gravitasi.v20i1.15517.

McGarry, C. K.; L. J. Grattan; A. M. Ivory; F. Leek; G. P. Liney; Y. Liu and C. H. Clark. (2020). Tissue mimicking materials for imaging and therapy phantoms: a review: Physics in Medicine & Biology, 65(23). https://doi.org/10.1088/1361-6560/abbd17.

McKee, C.T.; J.A. Last; P. Russell and C.J. Murphy. (2011). Indentation versus tensile measurements of Young's modulus for soft biological tissues. Tissue Engineering Part B: Reviews, 17(3): 155-164. https://doi.org/10.1089%2Ften.teb.2010.0520.

Meilinda, T.; E. Hidayanto and Z. Arifin. (2014). Pengaruh Perubahan Faktor Eksposi Terhadap Nilai CT Number. Youngster Physics Journal, 3(3): 269-278 https://ejournal3.undip.ac.id/index.php/bfd/article/view/5945.

Mufida, W.; A. P. Utami and S. N. Dewi. (2020). Pembuatan Phantom Radiologi Berbahan Dasar Kayu Lokal sebagai Pengganti Tulang Manusia, Jurnal Imejing Diagnostik , 6(1): 7-10 https://doi.org/10.31983/jimed.v6i1.5404.

Park, S. Y.; C. H. Choi; J. M. Park; M. Chun; J. H. Han and J. I. Kim. (2016). A patient-specific polylactic acid bolus made by a 3D printer for breast cancer radiation therapy. PloS one, 11(12): e0168063 https://doi.org/10.1371/journal.pone.0168063.

Purwantiningsi, P. and Lesmana, H. (2019). Pengukuran Nilai CT Number Pada Phantom CIRS 062m sebagai Data Input Kalkulasi Dosis Program ISIS 3D di Treatment Planning System. Jurnal Ilmiah Giga, 17(2): 70-78 http://journal.unas.ac.id/giga/article/viewFile/541/428.

Saito, M. and S. Sagara. (2017). A simple formulation for deriving effective atomic numbers via electron density calibration from dual-energy CT data in the human body. Medical Physics, 44(6): 2293-2303. https://doi.org/10.1002/mp.12176.

Sari, D. A.; E. Setiawati and Z. Arifin. (2018). Analisis Nilai Computed Tomography Dose Index (CTDI) Phantom Kepala Menggunakan CT Dose Profiler Dengan Variasi Pitch. Berkala Fisika, 23(2): 42-48. https://ejournal.undip.ac.id/index.php/berkala_fisika/article/view/30622.

Seeram, E. (2016). Computed Tomography: Physical Principles. Clinical Applications, And Quality Control, Fourth. Vol. Fourth. St. Louis, Missouri: Elsevier.

Sicard, D.; A. J. Haak; K. M. Choi; A. R. Craig; L. E. Fredenburgh and D. J. Tschumperlin. (2018). Aging and anatomical variations in lung tissue stiffness. American Journal of Physiology-Lung Cellular and Molecular Physiology, 314(6): L946-L955. https://doi.org/10.1152/ajplung.00415.2017.

Yunus, B. and B. Murtala. (2010). Pemanfaatan hounsfield unit pada CT-scan dalam menentukan kepadatan tulang rahang untuk pemasangan implan gigi, Journal of Dentomaxillofacial Science, 9(1): 34-38. https://jdmfs.org/index.php/jdmfs/article/view/230.

Zhang, F.; H. Zhang; H. Zhao; Z. He; L. Shi and Y. He. (2019). Design and fabrication of a personalized anthropomorphic phantom using 3D printing and tissue equivalent materials. Quantitative imaging in medicine and surgery, 9(1): 94-100. https://doi.org/10.21037%2Fqims.2018.08.01.